



# High-Efficiency Oxidant-Free Leaching of Rhenium from Arsenic–Rhenium Filter Cake

SHENGHANG XU,<sup>1</sup> YUKUN SHEN,<sup>1</sup> TANNA YU,<sup>1</sup> HUIBIN ZHANG,<sup>1</sup>  
HUAZHEN CAO,<sup>1</sup> and GUOQU ZHENG<sup>1,2</sup>

1.—College of Material Science and Engineering, Zhejiang University of Technology, Hangzhou 310014, Zhejiang, China. 2.—e-mail: zhengq@zjut.edu.cn

Arsenic–rhenium filter cake, one of the main wastes produced by copper smelting systems, is a vital source of rhenium (Re). Using traditional hydrometallurgy methods, rhenium can be leached by sulfuric acid solution with the help of oxidants. However, the residual oxidants can seriously affect the efficiency and lifetime of the extractants and ion-exchange resins. We herein propose a novel method to leach rhenium through a displacement reaction using copper sulfate solution, thereby avoiding the use of oxidants. The results show that Re element exists in the arsenic–rhenium filter cake in two forms:  $\text{Re}_2\text{S}_7$  and (As,Re)S amorphous. The rhenium leaching efficiency can reach 93.18%, and the kinetic data fit the shrinking core model. The leaching rate is controlled first by chemical reaction, with an apparent activation energy of  $78.46 \text{ kJ mol}^{-1}$ . Afterwards, the leaching kinetics of rhenium fits an internal diffusion model. The results provide theoretical guidance on how to make full use of waste residues from copper smelting systems.

## INTRODUCTION

Rhenium (Re) has attracted increasing attention in recent decades as a strategic and rare metal.<sup>1</sup> Due to its high melting point, rhenium is considered to be an indispensable component of nickel-based superalloys that are utilized in turbine blades of jet engines.<sup>2</sup> Besides, rhenium is also widely used in the petrochemical industry as an important catalyst.<sup>3</sup> For example, platinum–rhenium catalysts are vital constituents applied in the refining process of high-octane hydrocarbons.<sup>4</sup> With the rapid development of the aerospace and petroleum industries, the demand for rhenium is expected to increase by 5% per year over the coming decades.<sup>5</sup> However, the content of rhenium in the Earth's crust is relatively limited, only approximately  $10^{-70}$ .<sup>6</sup> Moreover, no independent mineral deposits of rhenium have been discovered to date. Generally, rhenium is always associated with copper ores in the form of rhenium sulfide ( $\text{ReS}_2$ ,  $\text{Re}_2\text{S}_7$ ).<sup>7</sup> With the rapid development in this field, the total amount of associated rhenium entering copper

smelting systems increases. Therefore, methods to extract rhenium from copper smelting residues has attracted increasing attention recently.

To date, one of the main processes used to extract rhenium from copper smelting systems was the waste acid method.<sup>8</sup> Most of the rhenium is separated from the smelting system as rhenium heptoxide ( $\text{Re}_2\text{O}_7$ ) in the exhaust gas during roasting, melting, and converting processes. The rhenium heptoxide is then dissolved into the waste acid to form perrhenic acid ( $\text{HReO}_4$ ).<sup>9</sup> Extraction and ion exchange are the main methods used to extract rhenium from waste acid. However, owing to the large volume of waste acid and the low concentration of rhenium, the extracting efficiency is relatively limited and the cost rather high.<sup>10</sup> Some oxidation leaching methods have also been reported to leach rhenium from arsenic filter cake with low content of rhenium, such as high-pressure oxidation leaching and oxidation leaching by oxidant.<sup>11</sup> Generally, the high-pressure oxidation leaching process is demanding in terms of the equipment required, restricting its application. Oxidation leaching by oxidant seems to be a good method to leach rhenium, and the most common oxidant used is hydrogen peroxide ( $\text{H}_2\text{O}_2$ ).<sup>12</sup> However, as a dangerous chemical, hydrogen peroxide exhibits a strongly

corrosive nature, being harmful to the human body as well as equipment. Application of other oxidants, such as  $\text{Cl}_2$  and  $\text{HClO}_4$ , in the leaching process has also been reported,<sup>13</sup> but neither of these is optimal. Moreover, residual oxidants can seriously affect the efficiency and service life of extractants and ion-exchange resins.<sup>14</sup> Therefore, there is an urgent need to identify a simple and economical approach for rhenium extraction.

When adding sodium sulfide to waste acid, arsenic and rhenium elements precipitate to form arsenic filter cake. However, the concentration of rhenium is relatively limited. The arsenic filter cake is recycled to the smelting systems, enabling concentration of rhenium to above 2 wt%. Rhenium can then be leached from the arsenic cake, which is known as “arsenic–rhenium filter cake.” Large production capacity of rhenium extraction from arsenic–rhenium filter cake can already be achieved using small-scale equipment. However, little research has been carried out on the process of leaching rhenium from arsenic–rhenium filter cake.

We present herein a novel, simple, and economical approach to leach rhenium from arsenic–rhenium filter cake without adding any oxidants, which could be an alternative on industrial scale as well. Copper sulfate, which can be easily obtained from waste copper electrolyte, is first reported as an additive agent to leach rhenium through a displacement rather than oxidation reaction. Because the solubility of  $\text{CuS}$  is much lower than that of  $\text{Re}_2\text{S}_7$ , rhenium sulfide can dissolve in copper sulfate solution. It is worth mentioning that  $\text{CuS}$  can be recycled to the smelting system to recover copper and sulfur. Various experimental factors, such as the leaching temperature, initial copper ion concentration, leaching time, stirring speed, and solid-to-liquid ratio were optimized. Moreover, the leaching kinetics of rhenium was studied in detail, and the mechanism of the leaching process is discussed.

## EXPERIMENTAL PROCEDURES

### Chemicals and Reagents

The leaching solution comprised deionized water (6  $\text{M}\Omega$  cm), copper sulfate pentahydrate, and sulfuric acid. In the leaching solution, the concentration of copper ion ranged from 10  $\text{g L}^{-1}$  to 30  $\text{g L}^{-1}$ , while that of sulfuric acid was 2  $\text{mol L}^{-1}$ . Copper sulfate pentahydrate (purity > 99%) and sulfuric acid (concentration > 98%) were both of analytical reagent (AR) grade and purchased from Chinese Medicine. Arsenic–rhenium filter cake was provided by Jinlong Copper Industry Co., Ltd.

### Pretreatment of Arsenic–Rhenium Filter Cake

Arsenic–rhenium filter cake should be pretreated before the leaching process. Firstly, the arsenic–rhenium filter cake was washed using deionized water to remove sodium sulfate and other soluble

impurities. The resulting turbid liquid was then subjected to suction filtration, thereby obtaining wet arsenic–rhenium filter cake that was applied directly in the experiments. The percentage of water in the wet arsenic–rhenium filter cake can be calculated as

$$W_{\text{water}} = \frac{(W_w - W_d)}{W_w} \times 100\% \quad (1)$$

where  $W_{\text{water}}$  represents the water content, and  $W_w$  and  $W_d$  are the weight of the wet and dry filter cake, respectively. Here, 100 g wet filter cake was taken and dried in a drying oven for 24 h, and the obtained dry filter cake weighed 29.83 g ( $\pm 0.21$  g). Using Eq. 1, the water content of the wet arsenic–rhenium filter cake was calculated to be 70.17%. Supplementary Table S1 presents the elemental composition of the dry filter cake, where the mass fraction of Re is 2.20%.

### Apparatus and Instruments

During the process of leaching rhenium from arsenic–rhenium filter cake, continuous stirring of the reacted mixture was performed using a stirring bar. The stirring speed was accurately controlled by using an electric motor, while the leaching temperature was controlled by using a water bath.

The rhenium concentration in the solution was analyzed by using an x-ray fluorescence spectrometer (ARL ADVANTX, Thermo). After drying under vacuum, the arsenic–rhenium filter cake and the precipitates were characterized by scanning electronic microscopy (SEM, Zeiss Merlin, operated at 15 kV). Phase identification of the precipitates was performed by x-ray diffraction (XRD) analysis (RIGAKU D/Max 2550 PC) with a  $\text{Cu K}_\alpha$  source ( $\lambda = 1.54059 \text{ \AA}$ ) at 40 kV at room temperature.

### Optimization of Rhenium Leaching of Arsenic–Rhenium Filter Cake

Leaching experiments were performed in a partially closed 1-L three-necked flask in a well-ventilated fume hood. A snake-like condenser pipe was applied to condense and recycle the water vapor, to reduce the water evaporation. At an appropriate time, 2 mL leaching solution was taken then filtrated through a 0.4- $\mu\text{m}$  microporous filter membrane. The concentration of rhenium was then analyzed, and the leaching efficiency of rhenium calculated as

$$\% \text{ Leaching efficiency} = \frac{C_{\text{Re}} \times V_{\text{leaching}}}{M_{\text{element}} \times m_{\text{sample}} \times (1 - W_{\text{water}})} \times 100\% \quad (2)$$

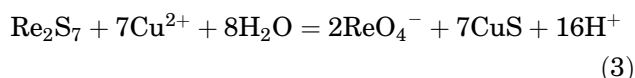
where  $C_{\text{Re}}$  and  $V_{\text{leaching}}$  are the concentration of rhenium and the total volume of leaching solution, respectively.  $M_{\text{element}}$  is the mass fraction of rhenium element in the dry filter cake, and  $m_{\text{sample}}$  represents the mass of the wet filter cake.

To optimize the leaching process, the initial copper ion concentration, solid-to-liquid ratio, stirring speed, and leaching temperature were systematically studied as experimental factors that can affect the leaching efficiency of rhenium from arsenic–rhenium filter cake. To guarantee the accuracy of the results and the conclusions, the experiments were repeated for three times for each group with different parameters.

## RESULTS AND DISCUSSION

### Thermodynamics Calculation

Because of the relatively limited solubility of CuS, the chemical reaction involved in leaching Re<sub>2</sub>S<sub>7</sub> can be described as



Based on thermodynamic calculations, the change in the Gibbs free energy ( $\Delta G$ ) for Eq. 3 at temperatures in the range from 0°C to 100°C is shown in Supplementary Fig. S1. The negative value of  $\Delta G$  for the reaction at the experimental temperatures (70–90°C) indicates that precipitation of Cu and dissolution of Re are thermodynamically feasible. It is easier to achieve the reaction with increasing temperature.

### Effect of Various Parameters on Leaching of Rhenium

#### Initial Copper Ion Concentration

To study the effect of the initial copper ion concentration on the leaching process, the leaching efficiency of rhenium was studied for different initial copper ion concentrations, and the leaching curves are shown in Fig. 1a. The leaching temperature was 90°C, the solid-to-liquid ratio was 100 g L<sup>-1</sup>, and the stirring speed was 400 rpm. When the initial copper ion concentration was increased from 10 g L<sup>-1</sup> to 20 g L<sup>-1</sup>, the Re leaching efficiency at 240 min increased from 47.35% to 88.16%, which can be explained by the limited availability of copper ion. If the copper ion concentration is relatively low (e.g., 10 g L<sup>-1</sup>), copper ion can be completely consumed, leading to low leaching efficiency. With further increase of the initial copper ion concentration (30 g L<sup>-1</sup>), the Re leaching efficiency reached 93.18%. Therefore, the optimum initial copper ion concentration of 30 g L<sup>-1</sup> was selected for subsequent experiments.

#### Solid-to-Liquid Ratio

The effect of the solid-to-liquid ratio on the rhenium leaching process was studied, as shown in Fig. 1b. The leaching process was conducted at the initial copper ion concentration of 30 g L<sup>-1</sup> with a stirring speed of 400 rpm at 90°C. The rhenium

leaching efficiency decreased with increasing solid-to-liquid ratio. The rhenium leaching efficiency was 87.65% and 94.89% when the solid-to-liquid ratio was 60 g L<sup>-1</sup> and 140 g L<sup>-1</sup>, respectively. These results indicate that decreasing the solid-to-liquid ratio favors a quick mass transfer rate between arsenic–rhenium filter cake and leaching solution. All the leaching curves reached a plateau state at approximately 120 min, with a rapid rate independent of the solid-to-liquid ratio, suggesting a change in the rate-limiting mechanism.<sup>15</sup> Copper ion is constantly consumed during the leaching process, but its concentration was still very high after 120 min. Indeed, the copper ion concentration remained above 18 g L<sup>-1</sup> after 120 min when the solid-to-liquid ratio was 60 g L<sup>-1</sup>. Meanwhile, the Re leaching efficiency was above 80%, illustrating that most of the rhenium sulfide in the arsenic–rhenium filter cake was continuously and severely consumed during the leaching process. After 120 min, the residual rhenium sulfide was insufficient to support such a high leaching rate, leading to its sharp decrease.

The Re leaching efficiency with a solid-to-liquid ratio of 60 g L<sup>-1</sup> was slightly higher than that at 100 g L<sup>-1</sup>, but the increase was marginal. Meanwhile, the lower the solid-to-liquid ratio, the greater the reagent volume required to leach the same amount of arsenic–rhenium filter cake, which is disadvantageous for industrialization. Thus, the solid-to-liquid ratio of 100 g L<sup>-1</sup> was taken as optimal.

#### Stirring Speed

The leaching process can be affected by the diffusion rate through the bulk to the solution, which in turn is determined by the stirring speed applied to the reaction mixture. Therefore, the effect of stirring speeds in the range from 200 rpm to 600 rpm on the Re leaching efficiency was investigated, as shown in Fig. 1c. The initial copper ion concentration was 30 g L<sup>-1</sup>, the solid-to-liquid ratio was 100 g L<sup>-1</sup>, and the leaching temperature was 90°C. When the stirring speed was 200 rpm, 400 rpm, and 600 rpm, the Re leaching efficiency after 240 min reached 71.29%, 93.18%, and 95.42%, respectively. However, there was almost no difference between the leaching rates at the stirring speeds of 400 rpm versus 600 rpm during the initial 60 min (fast leaching period), indicating that the effect of diffusion through the bulk could be ignored during the fast leaching period when the stirring speed exceeds 400 rpm. Therefore, considering energy saving, the stirring speed of 400 rpm was taken as optimal to guarantee sufficient agitation.

#### Leaching Temperature

To preserve the simplicity and economic advantage of the process, the leaching process is always applied under atmospheric pressure. Therefore, leaching temperatures from 70°C to 90°C were

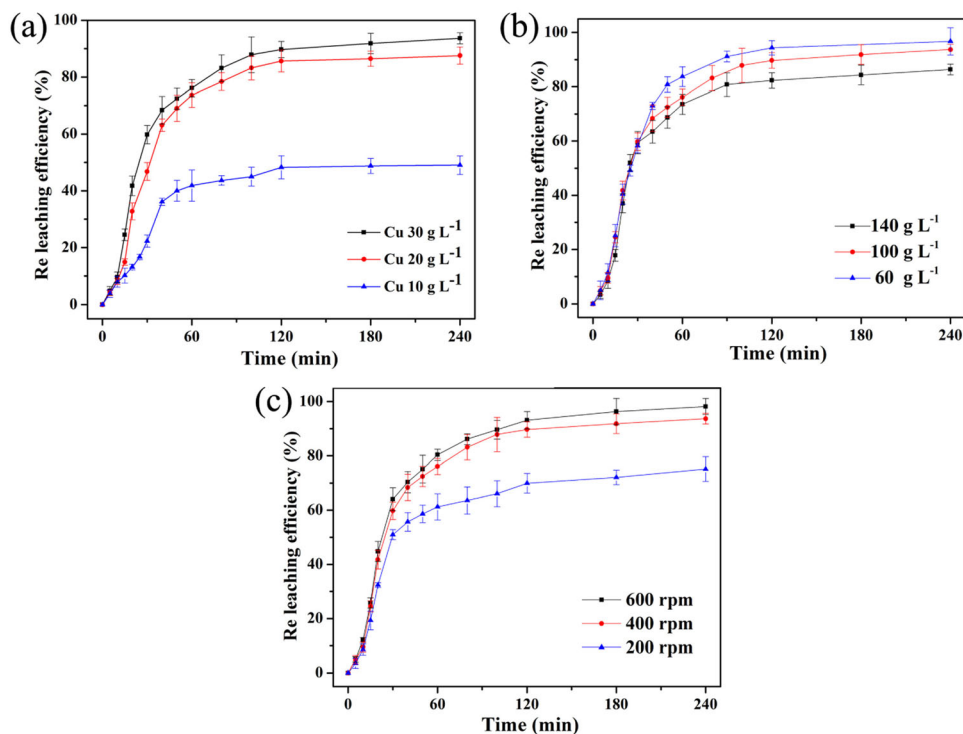


Fig. 1. Leaching curves of rhenium with different (a) initial copper ion concentrations, (b) solid-to-liquid ratios, and (c) stirring speeds.

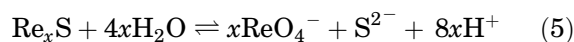
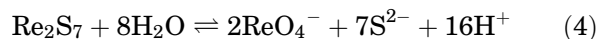
chosen to investigate their effect on the rhenium leaching efficiency (Fig. 2). Here, the leaching process was conducted at an initial copper ion concentration of  $30 \text{ g L}^{-1}$ , solid-to-liquid ratio of  $100 \text{ g L}^{-1}$ , and stirring speed of  $400 \text{ rpm}$ . The temperature affects the leaching process significantly, which is reflected in the following two aspects: leaching efficiency and leaching rate. Firstly, when the leaching temperature was increased from  $70^\circ\text{C}$  to  $90^\circ\text{C}$ , the Re leaching efficiency improved from  $68.92\%$  to  $93.18\%$ . Secondly, the leaching rate was also strongly dependent on the leaching temperature. Interestingly, in contrast to other leaching processes, the rhenium leaching rate in this work can be divided into four stages, where it is (I) relatively fast within the initial 10 min, (II) very slow thereafter, and (III) high again until reaching the final stage (IV), where it is extremely limited.

### Leaching Mechanisms

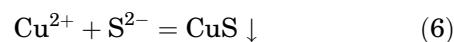
Figure 3 shows the microstructure of the arsenic–rhenium filter cake and the precipitates at different leaching times. As shown in Fig. 3a, the arsenic–rhenium filter cake consisted of nanoscale particles, indicating a large contact area between the filter cake and leaching solution. After leaching for 10 min at  $90^\circ\text{C}$ , some original CuS precipitates occurred with a long strip-like structure, as shown in Fig. 3b. After leaching for 40 min, the original CuS precipitates gradually grew to form a sheet-like structure. The unreacted arsenic–rhenium filter

cake was loosely covered by such interlaced CuS precipitates, as shown in Fig. 3c. As the reaction progressed, the solution constantly infiltrated through the CuS precipitates to react with the residual arsenic–rhenium filter cake. Finally, all the arsenic–rhenium filter cake was consumed, leaving only CuS precipitates. The XRD pattern of the residue after leaching at  $90^\circ\text{C}$  for 240 min is shown in Supplementary Fig. S3. Peaks corresponding to CuS can be indexed, directly proving the displacement reaction between arsenic–rhenium filter cake and copper sulfate solution. Besides, some unreacted components remained in the residues, such as  $\text{PbSO}_4$  and  $(\text{Pb,As})\text{S}$  sulfide.

The composition of the arsenic–rhenium filter cake is rather complex, and many reactions may occur during the leaching process. According to the XRD patterns shown in Supplementary Fig. S2(a), Re element existed in the arsenic–rhenium filter cake in two forms:  $\text{Re}_2\text{S}_7$  and  $\text{Re}_x\text{S}$  amorphous. In acid medium,  $\text{Re}_2\text{S}_7$  and  $(\text{As,Re})\text{S}$  amorphous can partly ionize as follows:



Because of the limited solubility of CuS, free copper ion can react with  $\text{S}^{2-}$  ion to form CuS precipitate as follows:





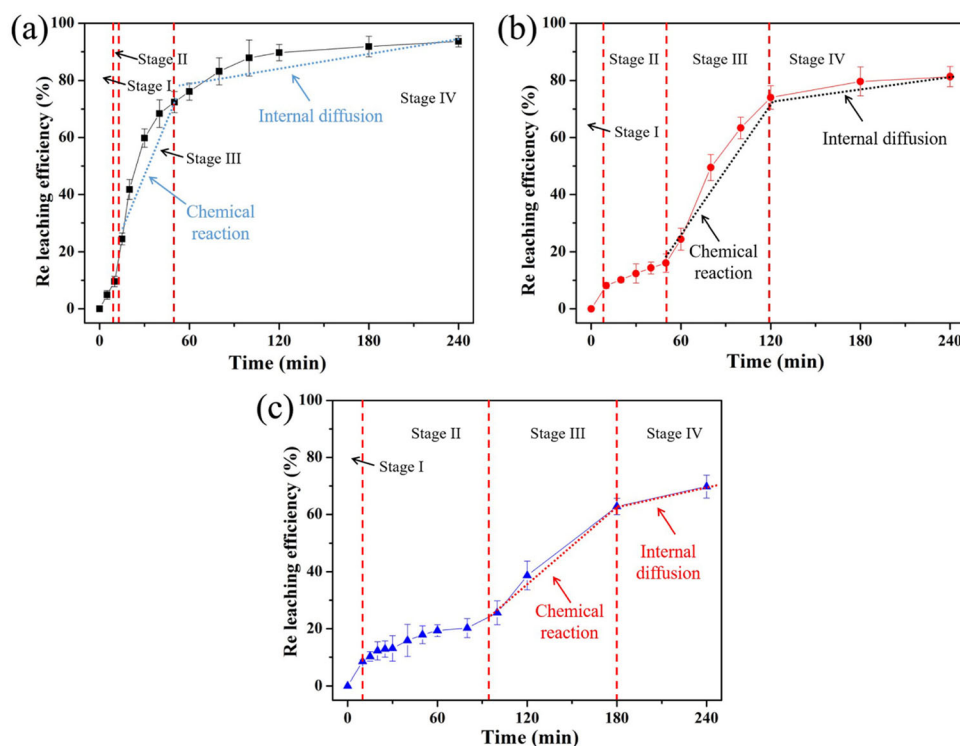


Fig. 2. Rhenium leaching curves at different leaching temperatures of (a) 90°C, (b) 80°C, and (c) 70°C; the dotted lines mark the different leaching stages.

When CuS precipitates are constantly formed, the concentration of  $S^{2-}$  ion drops, leading to further ionization of  $Re_2S_7$  and  $Re_xS$  amorphous to maintain the concentration of  $S^{2-}$ . Thus, the concentration of  $ReO_4^-$  ion increases while the Re leaching efficiency improves as the reaction progresses.

The leaching process can be divided into four stages, which can be clearly distinguished when leaching at 70°C, as shown in Fig. 2c. To separate out the effects of dissolution of  $Re_2S_7$  and  $Re_xS$  amorphous as well as the precipitation of CuS, the XRD patterns of residues after leaching for different periods are presented in Fig. 4, revealing that  $Re_xS$  amorphous was still present after 120 min while  $Re_2S_7$  phase was present even after 180 min. Besides, CuS phase was detected at the start of the leaching process, and its content was evidently increased after leaching for 120 min.

According to the XRD patterns in Fig. 4 and the leaching curves shown in Fig. 2c, the mechanisms of leaching rhenium from arsenic–rhenium filter cake in copper sulfate solution can be described as follows (Fig. 5): In the first stage (0 min to 10 min), the leaching temperature does not obviously affect the leaching rate, as shown by the similar slope of the rhenium leaching efficiency at different temperatures in Fig. 2. We can thus infer that the dissolution of acid-soluble (As,Re)S amorphous occurs in the acid medium first, as confirmed by the XRD patterns taken before and after a soaking

experiment in sulfuric acid solution in Supplementary Fig. S2. The transmission electron microscopy (TEM) images in Supplementary Fig. S4 show the microstructure of the acid-soluble  $Re_xS$  amorphous and the insoluble  $Re_xS$  amorphous, revealing that the particle size of insoluble  $Re_xS$  amorphous was about 30 nm while the acid-soluble  $Re_xS$  amorphous consisted of nanoscale particles. Moreover, we can infer that approximately 9% of the Re exists as acid-soluble amorphous in the arsenic–rhenium filter cake. The originally formed CuS precipitates lie loosely on the surface of the arsenic–rhenium filter cake. After the acid-soluble  $Re_xS$  amorphous has dissolved completely, the leaching rate becomes limited during stage II, which can be attributed to the oxidation layer. The arsenic–rhenium filter cake can be oxidized in air, thus consumption of the oxidation layer occurs first. The XRD patterns shown in Fig. 4 also confirm that the content of CuS precipitates did not change obviously during this period. The weak ionization of  $Re_2S_7$  and insoluble  $Re_xS$  amorphous then becomes dominant. The ionized  $S^{2-}$  ions are released from the filter cake and then quickly captured by  $Cu^{2+}$  (stage III). During this period, the CuS precipitates grow and transform to a sheet-like structure. Moreover, the solution can constantly infiltrate into the solid, thereby increasing the contact area between the arsenic–rhenium filter cake and solution, which leads to further release of  $S^{2-}$ . In the final stage, due to the exhaustion of  $Re_xS$  amorphous, as

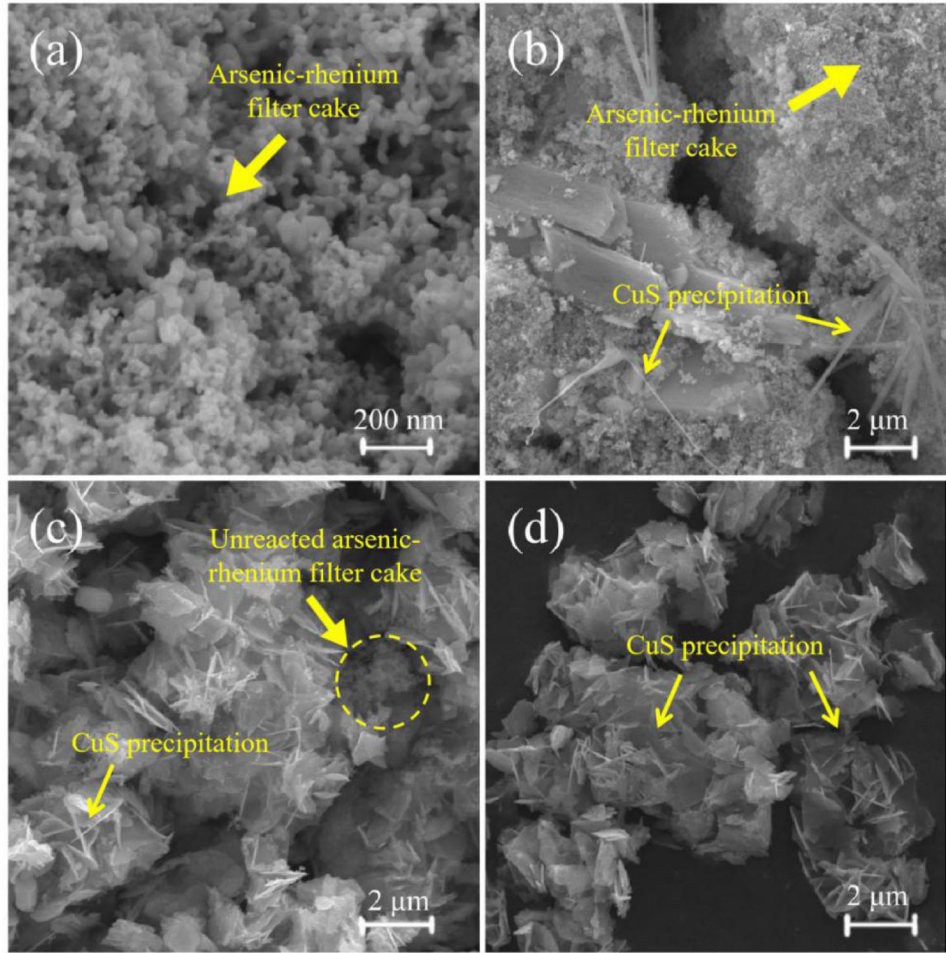


Fig. 3. Microstructure of (a) arsenic–rhenium filter cake before reaction and the residue after leaching at 90°C for different times: (b) 10 min, (c) 40 min, and (d) 240 min.

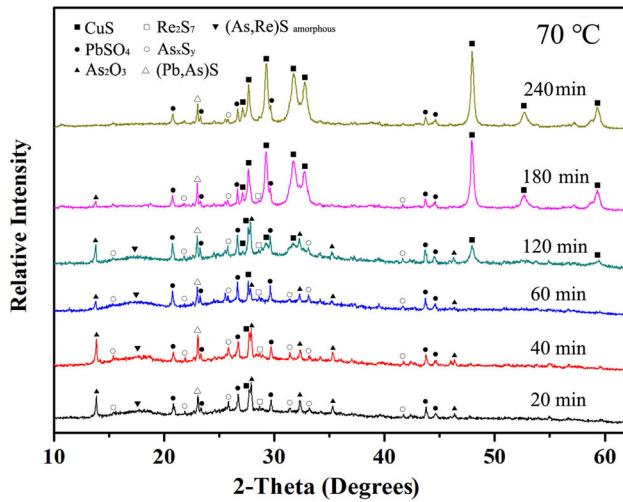


Fig. 4. XRD patterns of residues after leaching for different times at 70°C.

indicated in Fig. 4, the leaching rate becomes highly limited because of the consumption of the residual  $\text{Re}_2\text{S}_7$ . Thereafter, almost all the arsenic–rhenium

filter cake is consumed, and only sheet-like  $\text{CuS}$  precipitates remain.

### Leaching Kinetics of Rhenium

As mentioned above, dissolution of acid-soluble  $\text{Re}_x\text{S}$  amorphous and the oxidation layer occurs during leaching stages I and II. Here, we only discuss the leaching kinetics of rhenium from  $\text{Re}_2\text{S}_7$  and insoluble  $\text{Re}_x\text{S}$  amorphous in the arsenic–rhenium filter cake. As shown in Fig. 3, the arsenic–rhenium filter cake is loosely covered by  $\text{CuS}$  precipitates; the experimental data are analyzed using the shrinking core model.<sup>16</sup> Thus, the reaction rate may be controlled by surface chemical reaction, diffusion through a fluid film (external diffusion), or diffusion through a product layer (internal diffusion). The rate equations corresponding to these controlling mechanisms can be described as follows:<sup>17</sup>

Chemical reaction control:

$$1 - (1 - X)^{\frac{1}{3}} = k_1 t \quad (7)$$

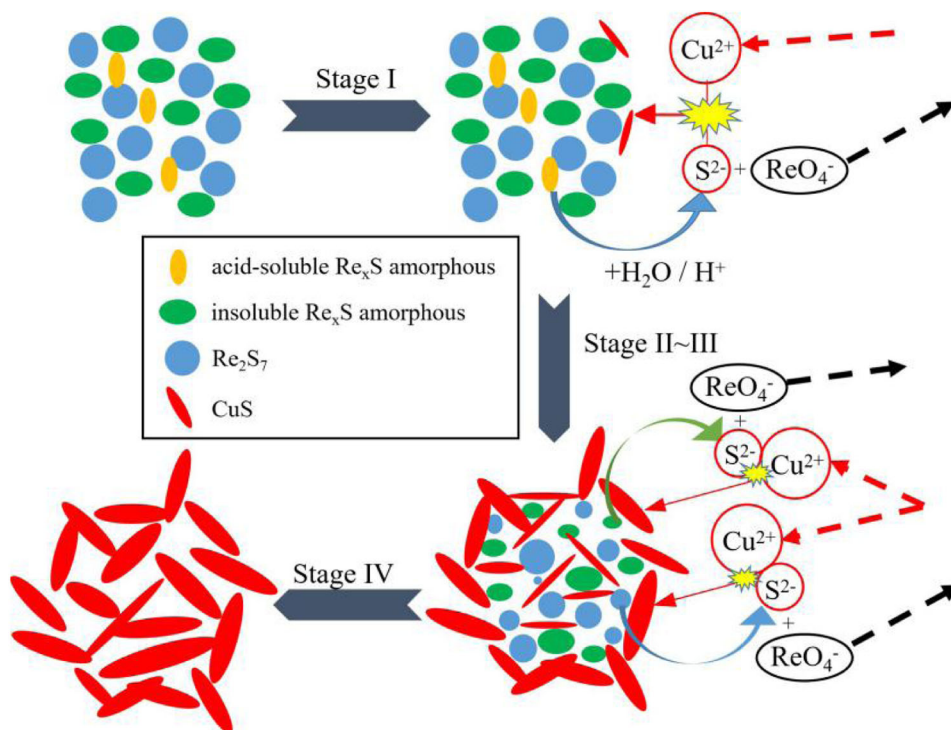


Fig. 5. Schematic diagram of leaching process.

External diffusion control:

$$1 - (1 - X)^{\frac{2}{3}} = k_2 t \quad (8)$$

Internal diffusion control:

$$1 - \frac{2}{3}X - (1 - X)^{\frac{2}{3}} = k_3 t \quad (9)$$

where  $X$  is the leaching efficiency;  $k_1$ ,  $k_2$ , and  $k_3$  are the apparent reaction rate constants for the chemical reaction, external diffusion, and internal diffusion control steps, respectively;  $t$  is the leaching time.

To determine the rate-limiting step in the leaching process, the experimental data from the leaching curves were transformed and fit to the equations above, and the correlation coefficient ( $R^2$ ) was used to evaluate the fitting precision.

The process of leaching rhenium from the arsenic–rhenium filter cake presents two types of leaching kinetics, and the correlation coefficients ( $R^2$ ) of the three kinetic models during the different leaching periods are presented in Supplementary Table S2. The experimental parameters were selected as follows: leaching temperature of 90°C, solid-to-liquid ratio of 100 g L<sup>-1</sup>, copper ion concentration of 30 g L<sup>-1</sup>, and stirring speed of 400 rpm. According to the leaching curve in Fig. 2a, the leaching process can be divided into two parts: a first part from 15 min to 40 min, and a second part from 40 min until the end. Based on the calculation,

the first part is governed by the rate of chemical reaction while internal diffusion dominates the other part. This outcome explains why the leaching rate decreases sharply after 40 min. The different models fit to the kinetic data and the correlation coefficients ( $R^2$ ) are presented in Supplementary Table S2 and Fig. 6.

To evaluate whether these two leaching mechanisms fit all the experimental conditions, the models were applied to fit the leaching curves obtained during the optimization of the initial copper ion concentration, solid-to-liquid ratio, and stirring speed. Figure 7 shows the linear fitting curves of the leaching mechanisms for variable initial copper ion concentration, solid-to-liquid ratio, or stirring speed. Two types of mechanisms are applied to clarify the entire leaching process, that is, the chemical reaction mechanism for the rapid leaching period and the internal diffusion mechanism for the slow leaching period. Note that the time when the mechanism changes is not the same under all the different experimental conditions. These fitting results show that the correlation coefficients are all greater than 0.9, except for the leaching process with an initial copper ion concentration of 10 g L<sup>-1</sup>, indicating excellent compatibility. The large deviation between the predicted and experimental results can be explained as follows: the copper ions are exhausted during the initial leaching period, thereby affecting the rhenium leaching efficiency in the internal diffusion period. The leaching efficiency of rhenium is only 47.35%.



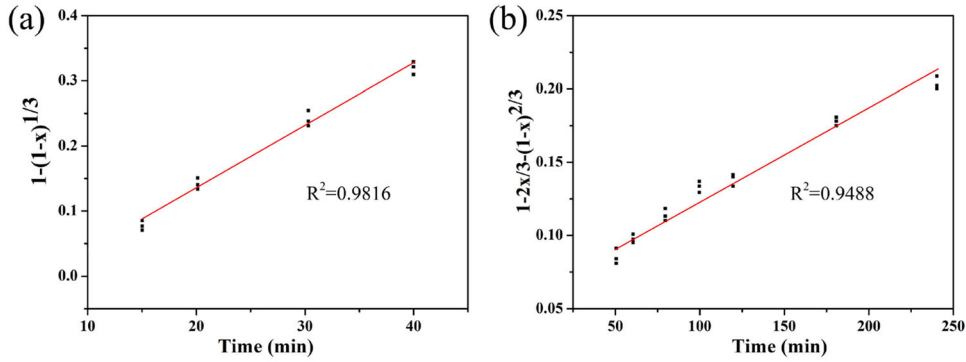


Fig. 6. Kinetics of leaching rhenium from the arsenic-rhenium filter cake as calculated by the shrinking core model when the leaching kinetic is (a) chemical reaction controlled at initial leaching period and (b) internal diffusion controlled thereafter.

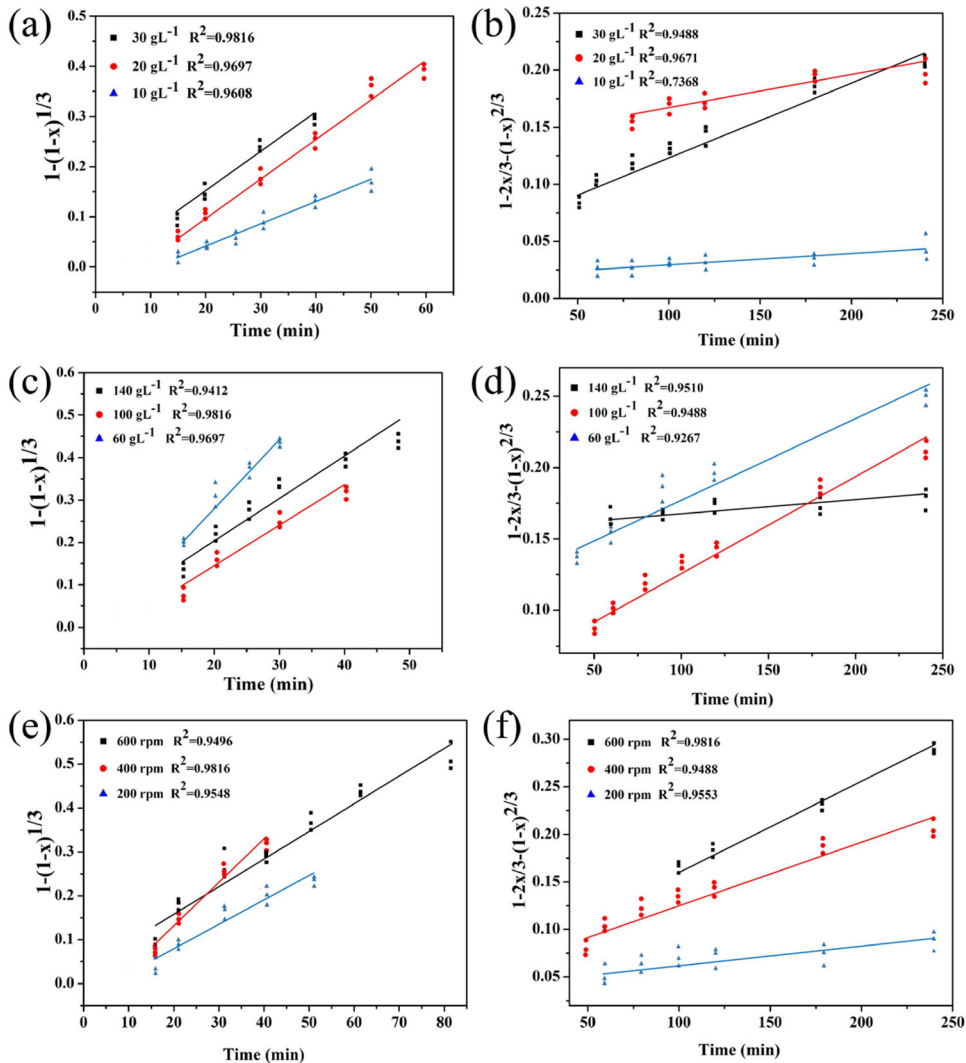


Fig. 7. Leaching kinetics models of rhenium with respect to variation in the concentration of copper ion controlled by (a) chemical reaction and (b) internal diffusion, solid-to-liquid ratio controlled by (c) chemical reaction and (d) internal diffusion; stirring speed controlled by (e) chemical reaction and (f) internal diffusion.

**Leaching Apparent Activation Energy**

To calculate the apparent activation energy of the leaching process, the chemical reaction model is

applied to describe the rapid leaching stage at different temperatures. It is well accepted that the internal diffusion rate is evidently lower than the chemical reaction rate.<sup>18</sup> It will take a long time,



maybe far more than 240 min, to reach the equilibrium state of the leaching process, especially at 70°C. Therefore, we concentrate our focus on critical reactions during this leaching period, and only the apparent activation energy of the chemical reaction model is calculated to guarantee the accuracy of the results. Figure 8a shows the linear fitting curves for the chemical reaction model with the correlation coefficients at different leaching temperatures, and Supplementary Table S3 lists the apparent reaction rate constants and correlation coefficients.

According to the Arrhenius equation,<sup>19</sup> the apparent rate constant can be described as

$$k = Ae^{-\frac{E}{RT}} \quad (10)$$

The logarithmic form of the Arrhenius equation is as follows:

$$\ln k = \ln A - \frac{E}{RT} \quad (11)$$

where  $k$  is the apparent rate constant,  $A$  is the preexponential factor, and  $E$ ,  $R$ , and  $T$  represent the apparent activation energy, the ideal gas constant, and the leaching temperature, respectively.

According to the slopes of the fitting curves,  $k$  values can be obtained, as shown in Supplementary Table S3. The apparent activation energy of the fast leaching period is calculated as 78.46 J mol<sup>-1</sup>, as shown in Fig. 8b. This value also clearly confirms that the fast leaching period is controlled by chemical reaction.<sup>12</sup>

Besides, the leaching rate of rhenium is significantly influenced by the initial copper ion concentration, as shown in Fig. 1a. According to the Arrhenius equation and the shrinking core model equation, the effect of the initial copper ion concentration can be described as<sup>20</sup>

$$1 - (1 - X)^{\frac{1}{3}} = k_1 t = k' C_{\text{Cu}^{2+}}^n t \quad (12)$$

and

$$k_1 = k' C_{\text{Cu}^{2+}}^n \quad (13)$$

Therefore, the logarithmic form of Eq. 13 can be expressed as

$$\ln k_1 = \ln k' + n \ln C_{\text{Cu}^{2+}} \quad (14)$$

where  $k'$  is the Arrhenius constant, which can be inferred from the intercept of the straight line in Fig. 8b;  $n$  is the empirical reaction order;  $C_{\text{Cu}^{2+}}$  (mol L<sup>-1</sup>) is the initial copper ion concentration in the leaching solution.

When the leaching temperature is 90°C (363 K), the reaction order of copper ion concentration can be calculated as the basis of Eq. 14, as shown in Fig. 8c. The linear correlation between the apparent rate constant ( $k$ ) and the initial copper ion concentration is excellent ( $R^2 = 0.9964$ ). The reaction order of the leaching process is calculated to be 0.979, and  $k'$  is 0.060312. Therefore, the kinetic equation for leaching arsenic–rhenium filter cake based on the leaching temperature and initial copper ion concentration can be expressed as

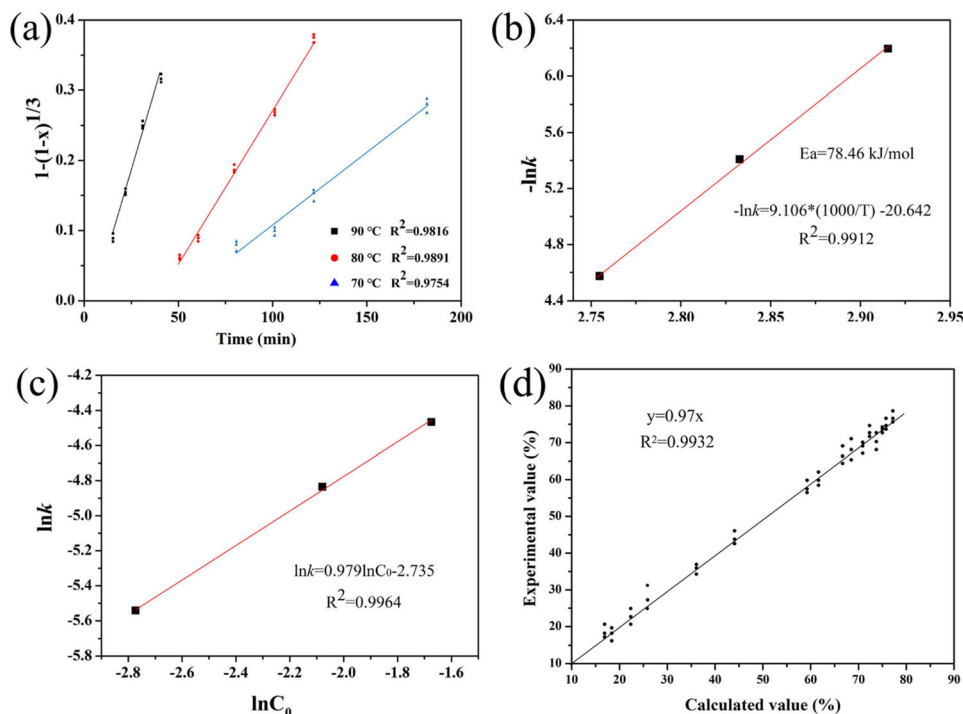


Fig. 8. (a) Plot of  $1 - (1 - X)^{1/3}$  versus time at different temperatures; (b) Arrhenius plot of leaching rhenium; (c) The relationship between  $\ln k$  and  $\ln C_{\text{Cu}^{2+}}$  at 90°C; (d) Comparison between experimental results for all the runs carried out in this study and those calculated by using Eq. 15.

$$1 - (1 - X)^{\frac{1}{3}} = 0.060312C_{\text{Cu}^{2+}}^{0.979} e^{-\frac{78.46 \times 1000}{RT}} t \quad (15)$$

Figure 8d shows a comparison between the experimental values of the Re leaching efficiency and those calculated by using Eq. 15. This indicates that the calculated kinetic equation agrees well with the experimental results. The above kinetic equation is helpful to optimize the process of leaching rhenium from arsenic-rhenium filter cake using a novel approach based on a displacement rather than oxidation reaction. Furthermore, it also provides theoretical guidance for making full use of waste residues from copper smelting systems by an efficient and economic method.

## CONCLUSION

A novel approach is proposed to leach rhenium from arsenic-rhenium filter cake. A displacement rather than oxidation reaction is utilized to achieve this high-efficiency leaching process. Several conclusions can be drawn as follows:

- (1) The optimal leaching efficiency of rhenium reaches 93.18% at the following conditions: leaching temperature of 90°C, leaching time of 4 h, initial copper ion concentration of 30 g L<sup>-1</sup>, solid-to-liquid ratio of 100 g L<sup>-1</sup>, and stirring speed of 400 rpm.
- (2) The shrinking core model is suitable for this leaching process, being controlled by two mechanisms: the chemical reaction mechanism for the rapid leaching period but the internal diffusion mechanism for the slow leaching period.
- (3) The process during the rapid leaching period is successfully described by the Arrhenius equation, with an apparent activation energy of 78.46 kJ mol<sup>-1</sup>. Based on data fitting and related calculations, the kinetic equation for leaching rhenium based on the leaching temperature and initial copper ion concentration can be expressed as

$$1 - (1 - X)^{\frac{1}{3}} = 0.060312C_{\text{Cu}^{2+}}^{0.979} e^{-\frac{78.46 \times 1000}{RT}} t$$

## ACKNOWLEDGEMENTS

This work was financially supported by the National Nature Science Foundation of China (Nos. 51874257 and 51374185).

## CONFLICT OF INTEREST

On behalf of all authors, the corresponding author states that there are no conflicts of interest.

## SUPPLEMENTARY INFORMATION

The online version of this article (<https://doi.org/10.1007/s11837-020-04560-3>) contains supplementary material, which is available to authorized users.

## REFERENCES

1. Z.W. Zhao and H.G. Li, *Metall. Mater. Trans. B.* 39, 519. (2008).
2. P. Raj, G. Singh, A.W. Thomas, and A. Scott, *Braymiller. Int. J Refract. Met. H.* 50, 79. (2015).
3. Y.Y. Shen, Y. Jiang, X.Y. Qiu, and S.L. Zhao, *JOM* 69, 1976. (2017).
4. Z.S. Abisheva, A.N. Zagorodnyaya, and N.S. Bekturganov, *Hydrometallurgy* 109, 1. (2011).
5. R.R. Srivastava, M.S. Kim, and J.C. Lee, *Ind. Eng. Chem. Res.* 55, 8197. (2016).
6. E.I. Gedgagov, S.V. Zakhar'yan, and D.V. Zakhar'yan, *Theor. Found. Chem. Eng.* 52, 912. (2018).
7. H.S. Kim, J.S. Park, S.Y. Seo, T. Tran, and M.J. Kim, *Hydrometallurgy* 156, 158. (2015).
8. E.E. Maltseva, A.A. Blokhin, Y.V. Murashkin, and M.A. Mikhaylenko, *Russ. J Non-ferr. Met.* 58, 463. (2017).
9. J. Yañez, S. Torres, D. Sbarbaro, R. Parra, and C. Saavedra, *IFAC-PapersOnLine* 51, 251. (2018).
10. S. Virolainen, M. Laatikainen, and T. Sainio, *Hydrometallurgy* 158, 74. (2015).
11. S.K. Mamo, M. Elie, M.G. Baron, A.M. Simons, and J. Gonzalez-Rodriguez, *Sep. Purif. Technol.* 212, 150. (2019).
12. A.O. Gezerman and B.D. Çorbacıoğlu, *Sur. Eng.* 31, 641. (2015).
13. A. Tuncuk, V. Stazi, A. Akcil, E.Y. Yazici, and H. Deveci, *Miner. Eng.* 25, 28. (2012).
14. S.V. Zakhar'yan and E.I. Gedgagov, *Theor. Found. Chem. Eng.* 47, 637. (2013).
15. F. Zhou, Q. Liu, J. Feng, J.X. Su, X. Liu, and R. Chi, *Sep. Purif. Technol.* 217, 24. (2019).
16. H.U. Sverdrup, A.H. Olafsdottir, K.V. Ragnarsdottir, and D. Koca, *BioPhys. Eco. Resour. Qual.* 3, 7. (2018).
17. O. Levenspiel, *Ind. Eng. Chem. Res.* 38, 4140. (1999).
18. S.S. Javaherian, H. Aghajani, and H. Tavakoli, *Miner. Process. Extra. M.* 127, 182. (2018).
19. M.R. Altıokka, H. Akalın, N. Melek, and S. Akyalçın, *Ind. Eng. Chem. Res.* 49, 12379. (2010).
20. M. Li, X.W. Zhang, Z.G. Liu, Y.H. Hu, M.T. Wang, J. Liu, and J.P. Yang, *Hydrometallurgy* 140, 71. (2013).

**Publisher's Note** Springer Nature remains neutral with regard to jurisdictional claims in published maps and institutional affiliations.